Int. J Heat Mass Transfer. Vol. 16, pp. 887–895. Pergamon Press 1973. Printed in Great Britain

HIGH REYNOLDS NUMBER FLUID DYNAMICS AND HEAT AND MASS TRANSFER IN REAL CONCENTRATED PARTICULATE TWO-PHASE SYSTEMS

I. YARON and B. GAL-OR
Department of Aeronautical Engineering, Technion—Israel Institute of Technology, Haifa, Israel

(*Received* 12 *November* 1971 *and in revised form* 28 *June* 1972)

Abstract—Correlations for high Reynolds number interfacial convective heat and mass transfer and fluid behaviour of real (i.e. not extraordinarily purified) concentrated two-phase systems of drops or bubbles are derived.

The theoretical results obtained compare favourably with various reported experimental data on separation angles, drag coefficients and Nusselt numbers.

NOMENCLATURE

a, radius of spherical particle;
c, concentration;
C_{D_v}, viscous drag coefficient;
C_{D_q}, form drag coefficient;
D, diffusivity;
D_p, form drag force;
D_v, viscous drag force;
f^{α}, function of Péclét number defined by equation (39);
F_T, parameter defined by equation (26);
$F(\mu, \rho)$, parameter defined by equation (16);
g, acceleration due to gravity;
G, parameter defined by equation (44);
K, parameter defined by equation (13);
m, distribution coefficient;
Nu, Nusselt number;
P, pressure;
Pe, Péclét number;
r, radial distance;
Re, Reynolds number defined by equation (19);
U_{rel}, average relative velocity between phases;
$\boldsymbol{V}$, velocity vector;
V, velocity component;
X, parameter defined by equation (43);
y, radial distance from interface, $y = r - a$;
Y, parameter defined by equation (18);
Z, parameter defined by equation (42).

Greek symbols

α^*, overall adsorption rate constant;
γ, "interfacial retardation viscosity";
Γ, surface concentration of surfactant impurities;
δ, boundary layer thickness;
ζ, parameter defined by equation (17);
η, dimensionless radial distance, $\eta = r/a$;
θ, polar angle;
θ_s, separation angle;
μ, dynamic shear viscosity;
ν, kinematic shear viscosity;
ρ, density;
σ, interfacial tension;
τ_{rr}, normal shear stress;
$\tau_{r\theta}$, tangential shear stress;
ϕ, volume concentration of dispersed phase;
$\chi(\theta)$, parameter defined by equation (15);
ψ, stream function;
α, vorticity.

Superscripts

c, denotes the continuous phase;
d, denotes the dispersed phase;
s, denotes surfactant impurities;
α, denotes the homogeneous phase considered;
$\mathring{}$, pertains to irrotational component;
$'$, pertains to viscous perturbation component;
$*$, dimensionless quantity;
$-$, average value.

Subscripts

b, refers to the bulk;
d, denotes the diffusional boundary layer;
f, denotes the hydrodynamic boundary layer;
i, value at interface;
r, radial component;
δ, refers to edge of boundary layer;
θ, tangential component;
ϕ, azimuthal component;
0, equilibrium value.

INTRODUCTION

IN DESIGNING of equipment and processes involving two-phase particulate systems, one often seeks an overall description of the fluid dynamics and interfacial heat and mass transfer rates. In such systems, contamination of fluid particle interfaces by the ever-present surfactant impurities, and the hydrodynamic interactions amongst neighbouring particles, are two major effects. The former causes retardation of internal circulation in fluid particles, thereby considerably reducing rates of interfacial transfer. Both effects have been considered by Yaron and Gal-Or [22], in their generalized analysis of slow viscous motion of ensembles of drops, bubbles, or solid particles in arbitrary imposed shear fields. The velocity profiles derived thereof for uniform fields have been used together with the Levich [11] "thin diffusional boundary layer" concept to calculate interfacial heat or mass transfer in such systems [18, 21].

An interesting numerical analysis of hydrodynamics and mass transfer in uncontaminated multibubble assemblages has been recently reported by LeClair and Hamielec [23] in a wide range of Reynolds numbers.

In the range of high particle Reynolds numbers Chao [4] and Moore [14], presented analytical solutions of the steady motion of single pure gas bubbles rising in a liquid. They represented viscous effects, restricted to a thin velocity boundary layer, as a perturbation imposed on an irrotational field. The boundary layer was shown to separate at the rear of the bubble, but the contribution of the region beyond the separation point was estimated to be insignificant. Winnikow and Chao [19] reported measured terminal velocities of single drops falling in a second liquid in carefully purified systems, and concluded that in such systems one cannot disregard altogether the effects of the separated flow region. The velocity fields obtained from the Chao–Moore theory have been incorporated by Winnikow [20], and Chen and Tobias [5], into their analyses of heat and mass transfer from single pure fluid particles at high Reynolds numbers.

The Chao–Moore analysis was also extended by Lochiel [12] to single bubbles with low levels of surface contamination, using Freündlich-type isotherms for surfactant adsorption.

The purpose of the present paper is to evaluate the applicability of the Chao–Moore theory to multiparticle (concentrated) systems with appreciable contamination levels, in light of available experimental data on separation angles, drag coefficients and Nusselt numbers.

FLOW DYNAMICS

In accordance with the Chao–Moore theory, the velocity vector $\boldsymbol{V}$ is considered to consist of irrotational $\mathring{\boldsymbol{V}}$ and viscous perturbation $\boldsymbol{V}'$ components, such that

$$\boldsymbol{V} = \mathring{\boldsymbol{V}} + \boldsymbol{V}'. \tag{1}$$

The hydrodynamic interactions amongst the neighbouring particles of an unbounded (i.e. with negligible wall effects) ensemble, are taken into account by means of the "spherical cell model", whose purely statistical nature is described elsewhere [7]. According to this model the entire ensemble is represented by a single typical particle enclosed in an imaginary spherical cell, whose dimensions are such that the particle-to-cell volume ratio equals the fractional volume of the dispersed phase ϕ in the entire ensemble [7]. Thus the disturbance to the external field due to the typical particle is restricted to the precincts of the cell. It should be emphasized that such models give statistically expected values for the velocity, temperature and concentration fields, which thus become *properties* of the entire ensemble. The LeClair and Hamielec [23] analysis is also based on the "spherical cell model", which, however, is subject to a different boundary condition, namely zero vorticity on the outer cell envelope.

Considering the motion of ensembles of drops or bubbles in uniform fields, placing now the origin of the coordinate system in the center of the "cell", and satisfying the cell-model requirements that the flow potential in the continuous phase attains the uniform imposed irrotational field values on the "cell" envelope, one readily obtains the following expressions for the irrotational velocity components:

$$\mathring{V}_r^c = -\frac{U_{rel}}{(1-\phi)}\left(1-\frac{1}{\eta^3}\right)\cos\theta, \tag{2}$$

$$\mathring{V}_\theta^c = \frac{U_{rel}}{(1-\phi)}\left(1+\frac{1}{2\eta^3}\right)\sin\theta, \tag{3}$$

$$\mathring{V}_r^d = \frac{3}{2}\frac{U_{rel}}{(1-\phi)}(1-\eta^2)\cos\theta, \tag{4}$$

$$\mathring{V}_\theta^d = \frac{3}{2}\frac{U_{rel}}{(1-\phi)}(1-2\eta^2)\sin\theta. \tag{5}$$

These expressions, which also represent the irrotational motion of two concentric spheres [13], were postulated by Ishii and Johnson [10] in their treatment of the motion of ensembles of slightly contaminated gas bubbles.

Introducing these expressions, together with equation (1) into the Navier–Stokes equations, neglecting the deviation from spherical shape of the fluid particle due to inertial effects, restricting the analysis to negligible effects of effluxing mass velocities on the flow field [24], assuming constant fluid properties, and neglecting terms by order-of-magnitude considerations, one arrives at the steady-state velocity boundary layer equation for tangential components

$$V_\theta^\alpha\cos\theta + \sin\theta\frac{\partial V_\theta^\alpha}{\partial\theta} - 2y\cos\theta\frac{\partial V_\theta^\alpha}{\partial y} = \frac{2}{3}\frac{av^\alpha}{U_{rel}}(1-\phi)\frac{\partial^2 V_\theta^\alpha}{\partial y^2}, \tag{6}$$

which holds for both phases.

This equation is solved with the following boundary conditions:

$$@\ r=\delta_f^c \qquad V_\theta^c = 0, \tag{7}$$

$$@\ r=\delta_f^d \qquad V_\theta^d = 0, \tag{8}$$

$$@\ r=a \qquad V_\theta^d = V_\theta^c, \tag{9}$$

$$@\ r=a \qquad \tau_{r\theta}^d - \tau_{r\theta}^c = (\partial\sigma/\partial\Gamma)\nabla_i\Gamma. \tag{10}$$

The last condition states that the difference between the tangential shear stresses in the continuous and dispersed phases at the interface of the typical particle are balanced by a dynamic interfacial tension force, which is due to surface concentration gradients of surfactant impurities. Employing the Levich–Newman [15] representation of the adsorption–desorption mechanism of surfactants at the interface, which is extensively discussed elsewhere [6], and utilizing equations (1)–(5) together with order-of-magnitude considerations, condition (10) becomes

$$\mu^d\frac{\partial V_\theta^d}{\partial r} - \mu^c\frac{\partial V_\theta^c}{\partial r} = 3\frac{U_{rel}}{a(1-\phi)}[\mu^c + \tfrac{2}{3}(\mu^d+\gamma)]\sin\theta, \tag{11}$$

where

$$\gamma = -\tfrac{1}{3}K\left(\frac{\partial\sigma}{\partial\Gamma}\right), \tag{12}$$

$$K = \frac{2\Gamma_0}{2D_i^s + \alpha^* D_b^s a^2/[D_b^s + \alpha^*\delta(\partial\Gamma/\partial C)_0]}. \tag{13}$$

One can regard γ as a sort of "interfacial viscosity", whose effect is to retard internal circulation within the typical fluid particle.

Using standard integral transform methods [4, 14], and satisfying boundary conditions (7)–(9) and (11), one obtains the following statistically expected average values of the tangential perturbation velocity components in both phases

$$V_\theta^\alpha = -6U_{\text{rel}}\sqrt{\left[\frac{2}{(1-\phi)Re^c}\right]}\sin\theta\chi^{\frac{1}{2}}(\theta) \times F(\mu,\rho)\, i\,\text{erfc}\,\zeta^\alpha, \tag{14}$$

where

$$\chi(\theta) = \tfrac{2}{3}\csc^4\theta(\tfrac{2}{3} - \cos\theta + \tfrac{1}{3}\cos^3\theta), \tag{15}$$

$$F(\mu,\rho) = \left(1 + \frac{3}{2}\frac{1}{\beta}\right)\Big/\left[1 + \left(\frac{\rho^d}{\rho^c}\frac{\mu^d}{\mu^c}\right)^{\frac{1}{2}}\right], \tag{16}$$

$$\zeta^\alpha = \frac{Y^\alpha}{2\chi^{\frac{1}{2}}(\theta)}, \tag{17}$$

$$Y^\alpha = \frac{|y|}{a}\sqrt{\left[\frac{Re^\alpha}{2(1-\phi)}\right]}, \tag{18}$$

$$Re^\alpha = \frac{2aU_{\text{rel}}}{\nu^\alpha}, \tag{19}$$

and

$$\beta = \frac{\mu^c}{\mu^d + \gamma}. \tag{20}$$

From the continuity equation using the boundary condition

$$@\ r = a \qquad V_r^d = V_r^c = 0, \tag{21}$$

one obtains the expected average radial perturbation velocity components

$$V_r^\alpha = \frac{8}{3}\frac{U_{\text{rel}}}{Re^c}F(\mu,\rho)\left\{\left[\frac{1}{2} + \left(\frac{1-\cos\theta}{\sin^2\theta}\right)^2\right]\text{erf}\,\zeta^\alpha + \left[1 - \left(\frac{1-\cos\theta}{\sin^2\theta}\right)^2\right]\zeta^\alpha i\,\text{erfc}\,\zeta^\alpha\right\}. \tag{22}$$

Representing the pressure as also consisting of irrotational and viscous perturbation components, we obtain from the boundary-layer equation for the radial perturbation velocity, the expected average perturbation pressure distribution

$$\bar{p}^\alpha = \frac{48}{Re^c}\rho^\alpha\frac{U_{\text{rel}}^2}{(1-\phi)}F(\mu,\rho)\sin^2\theta\chi(\theta)\left[i^2\,\text{erfc}\,\zeta^\alpha - \frac{4(1-\phi)}{\sqrt{(3\pi Re^c)}}\sin^2\theta\chi(\theta)\,(i\,\text{erfc}\,\zeta^\alpha - 4i^3 \times \text{erfc}\,\zeta^\alpha)\right]. \tag{23}$$

Using equations (2)–(5), (14) and (21) one derives formulae for the expected average dimensionless vorticity distributions and stream functions

$$\frac{\omega_\phi^\alpha a(1-\phi)}{U_{\text{rel}}} = 3\sin\theta\left(\frac{1}{\eta} - 1\right) - \sqrt{\left[\frac{3(1-\phi)}{Re^c}\right]} \times \frac{F(\mu,\rho)}{\eta}\frac{F_T^{\frac{1}{2}}}{\sin\theta}\, i\,\text{erfc}\,\zeta^\alpha - \frac{4}{3}\frac{(1-\phi)}{Re^c}\frac{F_T}{\eta} \times \frac{(1-\cos\theta)^3}{\sin^5\theta}(\text{erf}\,\zeta^\alpha - 2\zeta^\alpha i\,\text{erfc}\,\zeta) - F(\mu,\rho) \times \sqrt{\left[\frac{(1-\phi)}{3Re^c}\right]}\left(1 - \frac{1}{\eta}\right) \times \frac{2\sin\theta\cos\theta F_T^{\frac{1}{2}} - \frac{1}{2}\sin^5\theta}{F_T^{\frac{3}{2}}} \cdot \times \left\{\left[\frac{1}{2} + \left(\frac{1-\cos\theta}{\sin^2\theta}\right)^2\right]\frac{e^{-\zeta^{\alpha 2}}}{\sqrt{\pi}} + \left[1 - \left(\frac{1-\cos\theta}{\sin^2\theta}\right)^2\right](i\,\text{erfc}\,\zeta^\alpha - \zeta^\alpha \times \text{erfc}\,\zeta^\alpha)\right\} + \tfrac{3}{4}F(\mu,\rho)\sin\theta\,\text{erfc}\,\zeta^\alpha, \tag{24}$$

$$\frac{\psi^{\alpha}(1-\phi)}{a^2 U_{\text{rel}}} = \frac{3}{2}\frac{y}{a}\sin^2\theta + \frac{12}{Re^c}F(\mu,\rho)\sin^2\theta\chi(\theta) \times \left\{ i^2 \operatorname{erfc}\zeta^{\alpha} - \frac{4(1-\phi)}{\sqrt{(3\pi Re^c)}}\sin^2\theta\chi(\theta) \times (i\operatorname{erfc}\zeta^{\alpha} - 4i^3\operatorname{erfc}\zeta^{\alpha}) \right\} \quad (25)$$

$$F_T = \tfrac{2}{3} - \cos\theta + \tfrac{1}{3}\cos^3\theta. \quad (26)$$

SEPARATION ANGLES

All these expressions hold for the region anterior to the point of boundary layer separation. The separation angle θ_s can be evaluated from the consideration that for fluid particles the surface tangential velocity must reverse beyond the point of separation. Winnikow and Chao [13] present data on measured separation angles for both highly-purified and naturally contaminated single nitrobenzene drops, steadily falling in water (reproduced in Fig. 1). For pure

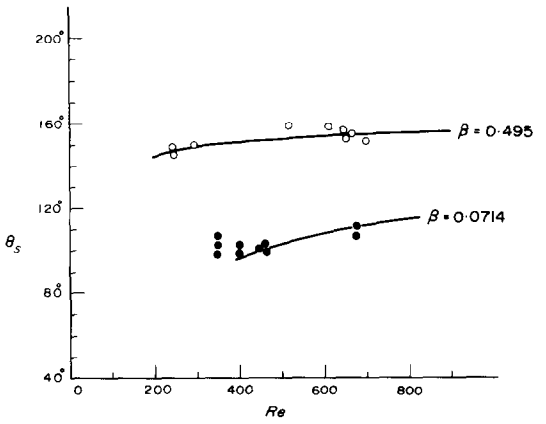

FIG. 1. Theoretical and experimental separation angles. Data of Winnikow and Chao [19] for single nitrobenzene drops, freely falling in water. Open circles—purified system; closed circles—contaminated system.

drops they have already noted agreement between theoretical predictions and the experimental data. However, for contaminated drops they did not provide a theoretical correlation with their data. In the absence of information on the extent of contamination in their system, we assign different values to the viscosity ratio parameter β, until we find a specific value (in this case 0·0714 as against 0·495 for a purified system), which quite adequately correlates the empirical data. These results seem to indicate that interfacial contamination by surfactant impurities tends to bring the point of separation closer to the front stagnation point and thus to give more emphasis to the region of separated flow.

DRAG ESTIMATION

With the aid of

$$D_v = 2\pi a^2 \int_0^{\theta_s} [(\tau^c_{r\theta})_a \sin\theta - (\tau^c_{rr})_a \cos\theta]\sin\theta\, d\theta, \quad (27)$$

$$D_p = 2\pi a^2 \int_0^{\theta_s} (p^c)_a \cos\theta \sin\theta\, d\theta, \quad (28)$$

we estimate expected average viscous and form drag coefficients:

$$C_{D_v} = \frac{16(1-\phi)}{Re^c}\left\{1 - \tfrac{3}{4}\cos\theta_s\left(1 + \frac{\cos^2\theta}{3}\right) - \frac{18}{5}F(\mu,\rho)\sqrt{\left[\frac{(1-\phi)}{3\pi Re^c}\right]}\left[1 - \frac{\sqrt{3}}{12} \times (2+\cos\theta_s)^{\frac{1}{2}} + \frac{5\sqrt{3}}{12}\cos\theta_s(2+\cos\theta_s)^{\frac{1}{2}}\right]\right\} + \frac{9\pi}{2F(\mu,\rho)}\left[1 - \frac{1}{F(\mu,\rho)}\right]\sin^4\theta_s, \quad (29)$$

$$C_{D_p} = \sin^2\theta_s - \frac{9}{8}\sin^4\theta_s + \frac{8F(\mu,\rho)(1-\phi)}{Re^c} \times \left\{\ln\left(\frac{1+\cos\theta_s}{2}\right) - \cos\theta_s + \frac{\cos^3\theta_s + 5}{6} - \frac{8}{45}\sqrt{\left[\frac{(1-\phi)}{\pi Re^c}\right]}\left[\frac{2(\cos\theta_s+2)^{\frac{1}{2}}}{(\cos\theta_s+1)} \times (\cos\theta_s - 4) + 3^{\frac{7}{2}}\right]\right\}. \quad (30)$$

One must stress that these expressions underestimate drag coefficients in comparison with experimental values, since they do not account for the region beyond the angle of separation. Nevertheless, one finds reasonable qualitative agreement between the theoretical predictions and Hamielec's [8] experimental data (Fig. 2), by again using arbitrary assumed values of β.

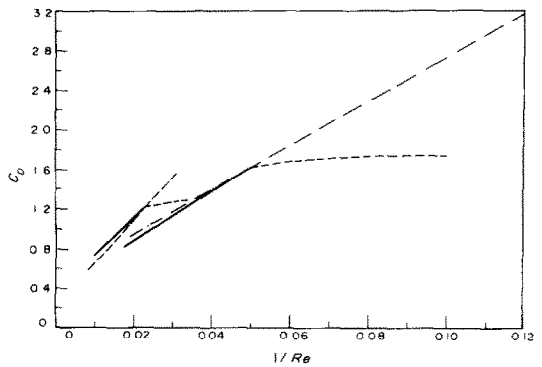

FIG. 2. Theoretical and experimental drag coefficients. Data of Hamielec [8] for systems: ——— n-butyl lactate–water ($\mu^d/\mu^c = 0{\cdot}266$, $\rho^d/\rho^c = 0{\cdot}8818$) and –.–.– paraldehyde–water ($\mu^d/\mu^c = 1{\cdot}06$, $\rho^d/\rho^c = 0{\cdot}9923$). Theoretical predictions (assumed values of γ/μ^c: for n-butyl-lactate–water—0·8, for paraldehyde–water $\gamma/\mu^c = 2{\cdot}0$ are shown as solid lines.

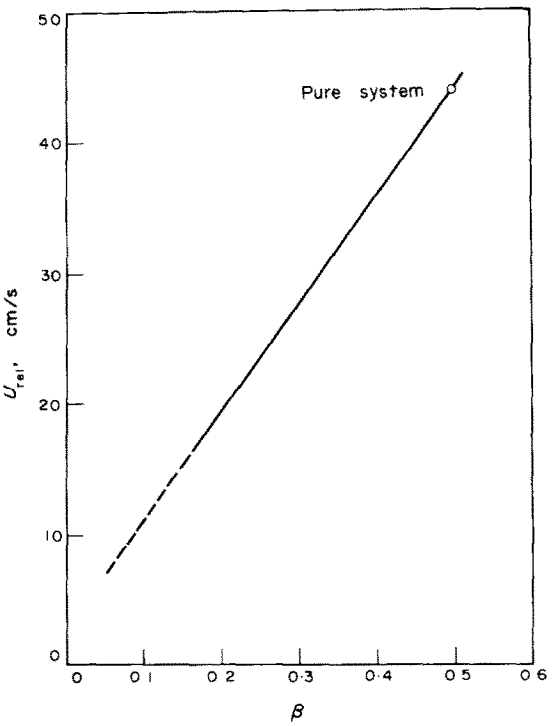

FIG. 3. Dependence of terminal velocity on viscosity parameter. System: Nitrobenzene drops in water ($\mu^d/\mu^c = 2{\cdot}02$, $\rho^d/\rho^c = 1{\cdot}203$, $a = 0{\cdot}14$ cm, $\phi = 0$).

It is possible, with the aid of equations (29) and (30), to approximately estimate the average relative velocity between the phases U_{rel}. This is obtained by applying a force balance to a freely falling typical particle, i.e.

$$D_v + D_p - \tfrac{4}{3}\pi a^3(\rho^d - \rho^c)(1 - \phi)g = 0. \quad (31)$$

This force balance contains two unknown quantities: the average relative velocity U_{rel} and the separation angle θ_s. These two quantities are also related through the expression for the surface average tangential velocity component V_θ^α when the condition $V_\theta^\alpha = 0$ at $\theta = \theta_s$ is satisfied. Thus the relative velocity U_{rel} and the separation angle θ_s are obtained by a simultaneous solution of both equations using a modified least-squares (Levenberg method) numerical technique. The results for a typical nitrobenzene drop freely falling in water at different levels of interfacial contamination are shown in Fig. 3. These results indicate a considerable reduction in the terminal velocity with increasing interfacial contamination. One should not attach too much physical significance to the results in the very low β region, since here the particle tends to exhibit almost completely rigid behaviour, at which the order-of-magnitude considerations which lead to equation (6) are no longer valid.

Numerical calculations also show (Fig. 4) the dependence of U_{rel} upon the particle volume fraction ϕ. The effect of particle concentration on U_{rel} in the Stokesian region [6] is shown to be stronger than in the high Reynolds number. This difference in behaviour demonstrates the inherent differences in the mechanisms of information transfer (on the presence of other particles) between an essentially inviscid flow and a purely viscous one.

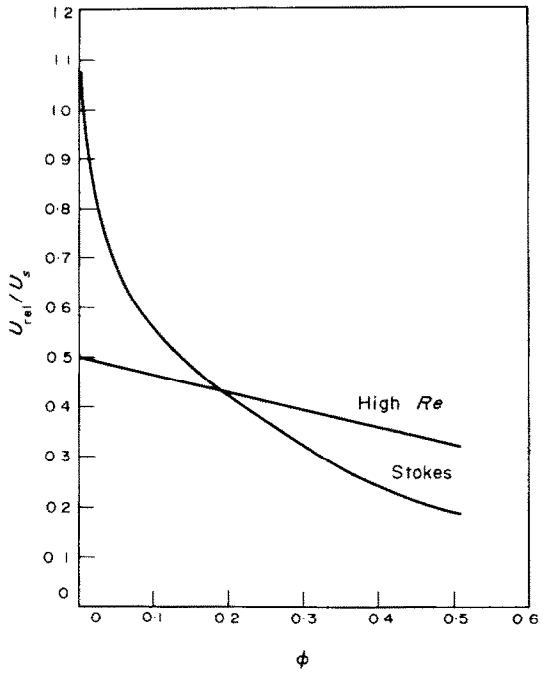

FIG. 4. Dependence of terminal velocity on volume fraction of dispersed phase. System: Nitrobenzene drops in water ($\mu^d/\mu^c = 2{\cdot}02$, $\rho^d/\rho^c = 1{\cdot}203$, $a = 0{\cdot}14$ cm, $\gamma = 0$). Relations for Stokesian range are also shown.

INTERFACIAL CONVECTIVE HEAT AND MASS TRANSFER

For binary diffusion with constant fluid properties, negligible effect of interfacial mass fluxes on the velocity field, and negligible distortion of the spherical fluid particle, the Levich [11] steady-state "thin-boundary layer" equation† for each phase in dimensionless form is

$$\overset{*}{V}{}_r^{\alpha}\frac{\partial \overset{*}{c}{}^{\alpha}}{\partial \eta} + \frac{\overset{*}{V}{}_{\theta}^{\alpha}}{\eta}\frac{\partial \overset{*}{c}{}^{\alpha}}{\partial \theta} = \frac{2}{Pe^{\alpha}}\frac{\partial^2 \overset{*}{c}{}^{\alpha}}{\partial \eta^2}, \tag{32}$$

where we define

$$Pe^{\alpha} \equiv \frac{2aU_{rel}}{(1-\phi)D^{\alpha}},$$

$$\overset{*}{c} \equiv \frac{c^{\alpha} - c_{\delta}^{\alpha}}{c_i^{\alpha} - c_{\delta}^{\alpha}},$$

$$\overset{*}{V}{}_r^{\alpha} \equiv \frac{V_r^{\alpha}(1-\phi)}{U_{rel}},$$

$$\overset{*}{V}{}_{\theta}^{\alpha} \equiv \frac{V_{\theta}^{\alpha}(1-\phi)}{U_{rel}}.$$

Solution of equation (32) is subject to satisfaction of the following boundary conditions:

$$@\ r = \delta_d^c \qquad \overset{*}{c}{}_{\delta}^{c} = 0, \tag{33}$$

$$@\ r = \delta_d^d \qquad \overset{*}{c}{}_{\delta}^{d} = 0, \tag{34}$$

$$@\ r = a \qquad \overset{*}{c}{}^{\alpha} = 1, \tag{35}$$

$$@\ r = a \qquad (\partial \overset{*}{c}{}^{\alpha}/\partial\theta)_{\theta=0} = (\partial \overset{*}{c}{}^{\alpha}/\partial\theta)_{\theta=\pi} = 0. \tag{36}$$

Expanding the dimensionless coordinate and concentration fields in a power series of Péclét numbers

$$\overset{*}{c}{}^{\alpha} = \overset{*}{c}{}_0^{\alpha} + f^{\alpha}c_1^{\alpha} + \ldots, \tag{37}$$

and

$$\frac{y}{a} = f^{\alpha}v^{\alpha} + \ldots, \tag{38}$$

where

$$f^{\alpha} = \sqrt{(2/Pe^{\alpha})}, \tag{39}$$

introducing the velocity components (2)–(5), (14) and (21), boundary layer equation (31) is brought to the form of the heat conduction equation by standard integral transforms [20], solving which one finally obtains

$$\frac{c^c - c_{\delta}^c}{c_{\delta}^d - mc_{\delta}^c} = \frac{(D^d/D^c)^{\frac{1}{2}}}{1 + m(D^d/D^c)^{\frac{1}{2}}}\,\mathrm{erfc}\,\frac{Z^c}{2\sqrt{X}}, \tag{40}$$

$$\frac{c^d - mc_{\delta}^c}{c_{\delta}^d - mc_{\delta}^d} = -\frac{1}{1 + m(D^d/D^c)^{\frac{1}{2}}}\,\mathrm{erfc}\,\frac{|Z^d|}{2\sqrt{X}}, \tag{41}$$

where

$$Z^{\alpha} = [1 - \cos^2\theta - GF_T^{\frac{1}{2}}]\frac{|y|}{a}, \tag{42}$$

† The analysis and formulations for convective heat transfer are similar and, therefore, will not be repeated here.

$$X = \frac{4}{3Pe^c}\left\{F_T + \frac{2G}{\sqrt{3}}\left[(2+\cos\theta)^{\frac{3}{2}} - \frac{(2+\cos\theta)^{\frac{5}{2}}}{5} - \frac{6\sqrt{3}}{5}\right]\right\}, \quad (43)$$

$$G = \frac{8}{\sqrt{(3\pi Re^c)}} F(\mu, \rho). \quad (44)$$

EXPERIMENTAL COMPARISONS OF NUSSELT NUMBERS

For the case of dominant resistance to transfer in the continuous phase the average diffusional Nusselt number is found to be given by

$$\overline{Nu^c} = \sqrt{\left(\frac{3Pe^c}{2\pi}\right)} \int_0^{\theta_s} \frac{(1-\cos^2\theta - GF_T^{\frac{1}{2}})\,d\theta}{\times\left\{F_T + \frac{2G}{\sqrt{3}}\left[(2+\cos\theta)^{\frac{3}{2}} - \frac{(2+\cos\theta)^{\frac{5}{2}}}{5} - \frac{6\sqrt{3}}{5}\right]\right\}^{\frac{1}{2}}}. \quad (45)$$

This expression reduces in the limits $\phi \to 0$ (single particle) and $Re^c \to \infty$ (irrotational motion) to the familiar results of Boussinesq [2] and Ruckenstein [17]:

$$\overline{Nu^c} = 1{\cdot}13\, Pe^{\frac{1}{2}}. \quad (46)$$

To obtain an analytical approximate expression for the average Nusselt number one can use the approximate relation due to Baird and Hamielec [1] (i.e. integrating over the entire surface of the particle rather than to the point of separation), here modified to read

$$\overline{Nu^c}\, Pe^{c-\frac{1}{2}} \cong \left[\frac{2(1-\phi)}{\pi U_{rel}} \int_0^{\pi} (V_\theta^c)_{y=0} \sin^2\theta\, d\theta\right]^{\frac{1}{2}}, \quad (47)$$

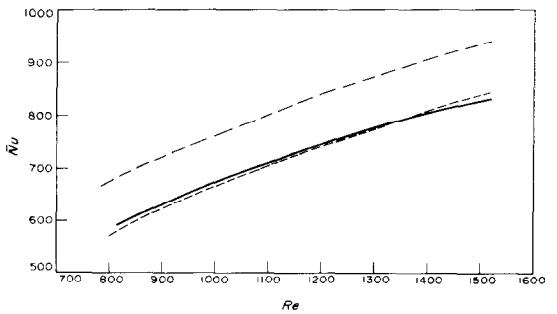

FIG. 5. Theoretical and experimental Nusselt numbers. —— Data of Bowman and Johnson [3]. -·- Theoretical, $F(\mu, \rho) = 1$. --- Theoretical, $F(\mu, \rho) = 5$.

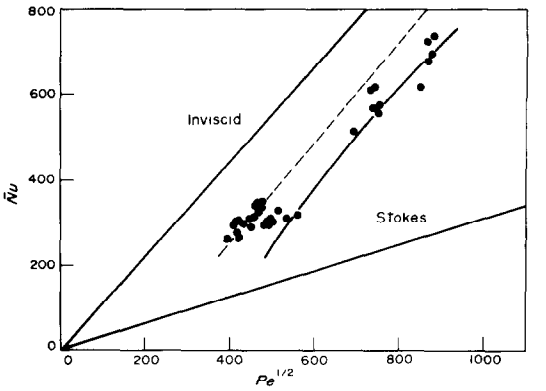

FIG. 6. Theoretical and experimental Nusselt numbers. ● Data of Heertjes *et al.* [9]. --- Theoretical, $\gamma = 0$. —— Theoretical, $\gamma = 6{\cdot}6$. Also shown are theoretical relations for inviscid [2] and Stokesian [21] ranges.

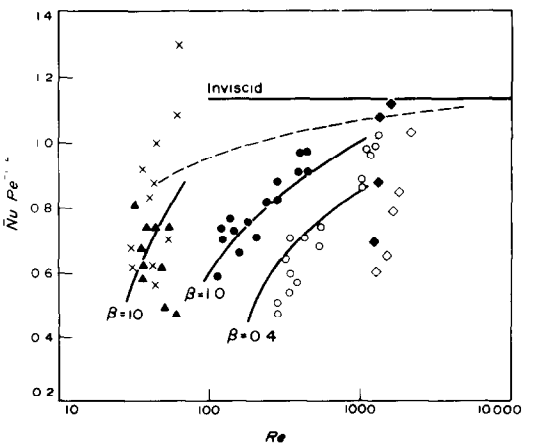

FIG. 7. Theoretical and experimental Nusselt numbers. Data of Redfield and Houghton [16]. --- Theoretical, $\gamma = 0$.

whereby we obtain

$$\overline{Nu}^c\, Pe^{c-\frac{1}{2}} \cong \frac{2}{\sqrt{\pi}}\left[1 - \frac{72}{5\sqrt{(3\pi Re^c)}} \times F(\mu, \rho)\left(1 - \frac{2\sqrt{3}}{9}\right)\right]^{\frac{1}{2}}, \quad (48)$$

which also reduces to (46) when $Re^c \to \infty$.

Using equation (48) and assigning different values to β, one can correlate in a satisfactory manner the experimental results of Bowman and Johnson [3] (Fig. 5), Heertjes *et al.* [9] (Fig. 6), and those of Redfield and Houghton [16] (Fig. 7). These comparisons emphasize the possible role of trace surfactant impurities in reduction of heat and mass transfer.

ACKNOWLEDGEMENTS

This work is supported by Grant No. 11–1196 from Stiftung Volkswagenwerk Research Foundation, Hannover, Germany. The authors gratefully acknowledge the work of Mr. M. Boazon who carried out part of the numerical computations.

REFERENCES

1. M. H. I. Baird and A. E. Hamielec, *Can. J. Chem. Engng* **40**, 119 (1960).
2. J. Boussinesq, *J. Math. Pure Appl.* **6**, 285 (1905).
3. C. W. Bowman and A. I. Johnson, *Can. J. Chem. Engng* **42**, 139 (1962).
4. B. T. Chao, *Physics Fluids* **5**, 19 (1962).
5. H. Y. Cheh and C. W. Tobias, *I/EC Fundamentals* **7**, 48 (1968).
6. B. Gal-Or and S. Walso, *Chem. Engng Sci.* **23**, 1431 (1968).
7. B. Gal-Or, *Can. J. Chem. Engng* **48**, 526 (1970).
8. A. E. Hamielec, Ph.D. Thesis, Univ. Toronto (1961).
9. P. M. Heertjes, W. A. Holve and H. Talsma, *Chem. Engng Sci.* **3**, 122 (1954).
10. T. Ishii and A. I. Johnson, *Can. J. Chem. Engng* **48**, 56 (1970).
11. V. G. Levich, *Physicochemical Hydrodynamics*, Prentice-Hall, Englewood Cliffs, N.J. (1962).
12. A. C. Lochiel, *Can. J. Chem. Engng* **43**, 40 (1965).
13. L. M. Milne-Thomson, *Theoretical Hydrodynamics*, McMillan, N.Y. (1957).
14. D. W. Moore, *J. Fluid Mech.* **16**, 161 (1963).
15. J. Newman, *Chem. Engng Sci.* **22**, 83 (1967).
16. J. A. Redfield and G. Houghton, *Chem. Engng Sci.* **20**, 131 (1965).
17. E. Ruckenstein, *Chem. Engng Sci.* **10**, 22 (1959).
18. S. Walso and B. Gal-Or, *Chem. Engng Sci.* **26**, 829 (1971).
19. S. Winnikow and B. T. Chao, *Physics Fluids* **9**, 50 (1966).
20. S. Winnikow, *Can. J. Chem. Engng* **46**, 217 (1968).
21. I. Yaron and B. Gal-Or, *Int. J. Heat Mass Transfer* **14**, 727 (1971).
22. I. Yaron and B. Gal-Or, *Rheologica Acta* (In press).
23. B. P. LeClair and A. E. Hamielec, *Can. J. Chem. Engng* **49**, 713 (1971).

DYNAMIQUE DES FLUIDES A GRAND NOMBRE DE REYNOLDS ET TRANSFERT THERMIQUE ET MASSIQUE DANS DES SYSTEMES BIPHASIQUES PARTICULAIRES CONCENTRES

Résumé On a établi des formules concernant le transfert interfacial de chaleur et de masse par convection à grand nombre de Reynolds et pour des systèmes de gouttes ou bulles réels biphasiques concentrés (cas d'un fluide peu purifié).

Les résultats théoriques obtenus se comparent favorablement aux différents résultats expérimentaux connus.

HYDRODYNAMISCHES VERHALTEN BEI HOHEN REYNOLDS-ZAHLEN UND WÄRME- UND STOFFÜBERTRAGUNG IN REALEN, KONZENTRIERTEN, ZWEIPHASIGEN SYSTEMEN MIT MAKROTEILCHEN

Zusammenfassung—Für hohe Reynolds–Zahlen werden Beziehungen abgeleitet für den konvektiven Wärme- und Stoffaustausch an der Phasengrenze und das Strömungsverhalten realer (d.h. nicht besonders gereinigter), konzentrierter zweiphasiger Systeme von Tröpfchen oder Blasen.

Die theoretischen Ergebnisse stimmen gut mit den experimentellen Daten anderer Autoren überein.

ГИДРОДИНАМИКА И ТЕПЛО- И МАССО-ПЕРЕНОС В РЕАЛЬНЫХ КОНЦЕНТРИРОВАННЫХ ДИСПЕРСНЫХ ДВУХФАЗНЫХ СИСТЕМАХ

Аннотация—Выводятся соотношения для конвективного тепло- и массо-переноса на поверхности раздела и поведения реальных (не очень чистых) концентрированных двухфазных систем, состоящих из капель или пузырьков, при больших числах Рейнольдса.

Полученные теоретические результаты хорошо согласуются с различными опубликованными эксперимента льными данными.